Naunyn-Schmiedeberg's Archives of Pharmacology (2023) 396:789–801
https://doi.org/10.1007/s00210-022-02358-5

RESEARCH

# Expression of ER stress markers (GRP78 and PERK) in experimental nephrotoxicity induced by cisplatin and gentamicin: roles of inflammatory response and oxidative stress

**Tuba Ozcan Metin[1] · Gulsen Bayrak[2] · Selma Yaman[3] · Adem Doganer[4] · Atila Yoldas[5] · Nadire Eser[6] · Duygun Altintas Aykan[6] · Banu Coskun Yilmaz[7] · Akif Hakan Kurt[8] · Lokman Ayaz[9] · Mehmet Sahin[10]**

Received: 4 October 2022 / Accepted: 29 November 2022 / Published online: 9 December 2022


## Abstract

This study aimed to establish the relationship between two endoplasmic reticulum (ER) stress proteins, glucose-regulated protein 78 (GRP78/BiP) and PKR-like endoplasmic reticulum kinase (PERK), and oxidative stress markers in cisplatin (CIS)–induced and gentamicin (GEN)–induced nephrotoxicity.

The study consisted of five groups: control (saline solution only), CIS D2 (2.5 mg/kg for 2 days), CIS D7 (2.5 mg/kg for 7 days), GEN D2 (160 mg/kg for 2 days), and GEN D7 (160 mg/kg for 7 days). All rats were sacrificed 24 h after the last injection for standard clinical chemistry, and ultrastructural and histological evaluation of the kidney.

CIS and GEN increased blood urea nitrogen (BUN) and serum creatinine (Cr) levels, as well as total oxidant status (TOS), while decreasing total antioxidant status (TAS) level in CIS D7 and GEN D7 groups. Histopathological and ultrastructural findings were also consistent with renal tubular damage. In addition, expression of markers of renal inflammation (tumor necrosis factor-α (TNF-α) and interleukin 1β (IL-1β)) and ER stress markers (GRP78 and PERK) was significantly increased in the kidney tissue of rats treated with CIS and GEN for 7 days.

These findings suggest that CIS and GEN administration for 7 days aggravates nephrotoxicity through the enhancement of oxidative stress, inflammation, and ER stress–related markers. As a result, the recommended course of action is to utilize CIS and GEN as an immediate but brief induction therapy, stopping after 3 days and switching to other drugs instead.

**Keywords** Nephrotoxicity · Cisplatin · Gentamicin · ER stress · GRP78/BiP · PERK

✉ Tuba Ozcan Metin
tubaozcanmetin@gmail.com; tubaozcanmetin@ksu.edu.tr

[1] Department of Histology and Embryology, Faculty of Medicine, Kahramanmaras Sutcu Imam University, Kahramanmaras, Turkey

[2] Department of Histology and Embryology, Faculty of Medicine, Usak University, Usak, Turkey

[3] Department of Biophysics, Faculty of Medicine, Kahramanmaras Sutcu Imam University, Kahramanmaras, Turkey

[4] Department of Biostatistics and Medical Informatics, Faculty of Medicine, Kahramanmaras Sutcu Imam University, Kahramanmaras, Turkey

[5] Department of Anatomy, Faculty of Medicine, Kahramanmaras Sutcu Imam University, Kahramanmaras, Turkey

[6] Department of Pharmacology, Faculty of Medicine, Kahramanmaras Sutcu Imam University, Kahramanmaras, Turkey

[7] Department of Histology and Embryology, Faculty of Medicine, Mersin University, Mersin, Turkey

[8] Department of Pharmacology, Faculty of Medicine, Bolu Abant Izzet Baysal University, Kahramanmaras, Turkey

[9] Department of Biochemistry, Faculty of Pharmacy, Trakya University, Edirne, Turkey

[10] Department of Medical Biology, Faculty of Medicine, Gaziantep University, Gaziantep, Turkey

## Introduction

Cisplatin (*cis*-diamminedichloroplatinum, CIS), an antineoplastic drug, is frequently used to treat solid tumors. In addition to its therapeutic benefits, it has serious side effects such as nephrotoxicity, neurotoxicity, ototoxicity, and hepatotoxicity (Manohar and Leung 2018; Ghosh 2019). CIS accumulates particularly in renal proximal tubule epithelial cells and causes cellular damage, and hence nephrotoxicity is supposed to be the primary side effect (Xu et al. 2015). The mechanisms of CIS-induced nephrotoxicity are associated with oxidative stress, apoptosis, inflammation, fibrogenesis, mitochondrial dysfunction, and endoplasmic reticulum (ER) stress (Yao et al. 2007; Inagi 2009).

Gram-negative bacterial infections are commonly treated with gentamicin (GEN), an aminoglycoside antibiotic (Balakumar et al. 2010). Tubular necrosis, tubular fibrosis, inflammation, renal failure, and a lower glomerular filtration rate are the mechanisms of GEN-induced kidney damage (Abd-Elhamid et al. 2018; Vysakh et al. 2018). Furthermore, oxidative stress is responsible for eventual cellular necrosis in renal tubules and thus plays a key role in GEN-induced nephrotoxicity (Balakumar et al. 2010).

Numerous cellular processes, such as protein folding, modification, and regulation of protein biosynthesis, occur in the ER. ER homeostasis is disrupted under a variety of physiological and pathological conditions, resulting in ER stress (Wei et al. 2021). Under stress circumstances, the ER's ability to fold proteins is reduced, which causes an accumulation of unfolded and improperly folded proteins in the ER lumen. Activating transcription factor 6 (ATF6), protein kinase R (PKR)–like endoplasmic reticulum kinase (PERK), and inositol-requiring protein 1 (IRE1) are the three primary ER stress sensors. Under normal circumstances, these sensors are coupled to binding immunoglobulin protein (BiP), also known as glucose-regulated protein 78 (GRP78), an ER-localized chaperone. When ER stress occurs, PERK dissociates from GRP78/BiP and activates eukaryotic initiation factor-2α (eIF2α), resulting in a decrease in the amount of proteins that can enter the ER (Foufelle and Fromenty 2016).

Although the mechanisms of CIS- and GEN-induced nephrotoxicity are not fully understood, the importance of increased oxidative stress and inflammatory cascades in many tissues has been highlighted. Several studies have shown that oxidative stress and inflammation are linked to ER stress (Jaikumkao et al. 2016; Hazman et al. 2018). Tumor necrosis factor-α (TNF-α)–induced inflammatory response increases intracellular oxidative stress and induces ER stress by increasing the expression level of ER sensor proteins such as PERK (Zhao et al. 2021). CIS treatment is reported to increase the expression of ER stress markers, such as PERK, IRE-1α, and CCAAT-enhancer binding protein homologous protein (CHOP), and inflammatory response markers (TNF-α and IL-1β) in HEK-293 and mouse kidney cells (Singh et al. 2018). In addition, the expression levels of calpain, caspase 12, GRP78, and CHOP proteins have been shown to increase significantly in GEN-induced nephrotoxicity, suggesting that GEN therapy causes ER stress and activates ER-mediated cell death markers (Jaikumkao et al. 2016).

There has been little research showing the effects of CIS and GEN treatment on ER stress. The goal of this study was to establish how two nephrotoxic drugs (CIS and GEN) affect the expression of GRP78 and PERK proteins, both of which are ER stress markers of oxidative stress, after 2 and 7 days of treatment.

## Materials and methods

### Animals and experimental design

The study involved 40 male Wistar rats (200–250 g). During the experiment, all of the rats were kept in a room that meets the requirements of an experimental animal laboratory (12 h light, 12 h dark cycle, constant temperature of 22 ± 3 °C). The Ethics Committee of Animal Research at Kahramanmaras Sutcu Imam University granted permission for the experimental protocol (Approval number: 2017/03–09). All experimental procedures were carried out in accordance with the National Institute of Health "Guide for the care and use of laboratory animals" rules.

Rats were divided into five groups and received the following treatments:

- Control ($n = 8$) received intraperitoneal (ip) injection of vehicle (0.9% NaCl solution).
- CIS D2 ($n = 8$) received ip injection of CIS (Kocak Farma, Turkey) at a dose of 2.5 mg/kg for 2 days.
- CIS D7 ($n = 8$) received ip injection of CIS at a dose of 2.5 mg/kg for 7 days.
- GEN D2 ($n = 8$) received ip injection of GEN (Genta, Ulagay, Turkey) at a dose of 160 mg/kg for 2 days.
- GEN D7 ($n = 8$) received ip injection of GEN at a dose of 160 mg/kg for 7 days.

Twenty-four hours after the last injection, rats were sacrificed for immunohistochemical, ultrastructural, and histopathologic evaluation of the kidney and blood samples were collected in tubes. The doses were prepared in accordance with earlier research that documented toxicity

and effectiveness in laboratory animals (Amin et al. 2004; Ozcicek et al. 2018).

### Histopathological analysis

The kidney tissues of rats were fixed in 10% formalin in phosphate buffer for 48 h before being processed by routine histological techniques and embedded in paraffin blocks. The sections (5 µm thickness) were prepared from the paraffin blocks using a rotary microtome (Leica, 2125RT) and stained with hematoxylin and eosin (H&E). Tubular damage was evaluated in ten fields for each slide at 200 × magnification as follows: 0 = none, 1 = ≤ 10%, 2 = 11–25%, 3 = 26–45%, 4 = 46–75%, and 5 = 76% (Malik et al. 2015).

### Immunohistochemical analysis

Sections taken on adhesive slides were deparaffinized and boiled in a microwave oven in Tris–EDTA buffer (100 ×, ab93684; Abcam) for antigen retrieval. The slides were then washed with phosphate-buffered saline (PBS) and treated with 3% hydrogen peroxide solution and blocked with normal goat serum (Invitrogen-50062Z). Anti-GRP78 BiP/HSPA5 (1:100, PB9640; Boster), anti-PERK (1:100, bs-2469R; Bioss), anti-TNF-α (1:100, ab6671; Abcam), and anti-IL-1β (1:100, ab9787; Abcam) primary antibodies were used to incubate the sections overnight at 4 °C. Following a PBS rinse, the sections were incubated with anti-rabbit IgG secondary antibody (1:200, 65–6140; Thermo Scientific) for 30 min at room temperature. The slides were then washed with PBS and incubated with horseradish peroxidase (HRP, 1:200, 43–4323; Thermo Scientific) for 10 min. The slides were placed in diaminobenzidine (DAB, ab64238; Abcam), then counterstained with Mayer's hematoxylin and mounted. For immunohistochemical evaluations, ten different fields were examined with a Carl Zeiss Axio Imager A2 microscope with a camera attachment at 200 × magnification and the staining intensity in each section was scored as strong (+ + + +), medium (+ + +), weak (+ +), or absent (+).

### Electron microscopy examination

After being fixed with 2.5% glutaraldehyde in 0.1 M phosphate buffer, the kidney tissue samples were postfixed with 1% osmium tetroxide, dehydrated using a graded alcohol series, cleaned with propylene oxide, and embedded in epon for transmission electron microscopy (TEM). An ultramicrotome (UCT-125; Leica Microsystems GmbH, Vienna, Austria) was used to cut ultrathin sections that were then contrasted with uranyl acetate and lead citrate. Finally, contrasted sections were analyzed and photographed using a TEM (JEM-1011; JEOL Ltd, Tokyo, Japan).

### Biochemical analysis

Blood samples, collected via cardiac puncture from sacrificed rats, were placed in serum-separating tubes. Following coagulation, serum samples were obtained by centrifugation at 3000 rpm for 10 min and stored at − 80 °C until biochemical examination. In a biochemistry autoanalyzer (Siemens Advia 1800 Chemistry Analyzer), blood urea nitrogen (BUN) and creatinine (Cr) levels were assessed using a spectrophotometric method. Total oxidant status (TOS) and total antioxidant status (TAS) in serum were analyzed using commercial colorimetric kits (Rel Assay Diagnostics, Turkey). TOS and TAS values were expressed as micromoles of $H_2O_2$ equivalent per liter and millimoles of Trolox equivalent per liter, respectively.

### Statistical analysis

Statistical analysis was conducted using R.3.3.2 software and IBM SPSS version 22 (IBM SPSS for Windows version 22; IBM Corporation, Armonk, New York, USA). The Shapiro–Wilk test was used to evaluate the data and determine whether the variables conformed to a normal distribution. One-way ANOVA was used to compare the differences between groups in variables with normal distribution. For normally distributed variables, pairwise comparison post hoc tests Tukey HSD test and Dunnett test (when variances were homogeneous), and Tamhane T2 test (when variances were not homogeneous) were used. The Levene test was used to determine the homogeneity of the variances. The Kruskal–Wallis *H* test was used to assess the differences in the variables that were not distributed normally between the groups. Assessment of variables that did not show normal distribution was performed with post hoc (pairwise comparisons) Dunn's test. Statistical significance was accepted as $p < 0.05$. Statistical parameters were expressed as mean ± SD and median (min–max).

## Results

### Histopathological examinations

The control group sections revealed that the tubules and glomeruli had typical morphology (Fig. 1a). The CIS D2 (Fig. 1b) and GEN D2 (Fig. 1e) groups showed minimal degeneration in the proximal tubules. In the CIS D7 group, however, atrophic glomeruli, necrotic cell debris spilled into the tubule lumen or degenerated epithelial cells, cellular vacuolization, hyaline casts, and inflammatory foci containing inflammatory cells were notable (Fig. 1c, d). The GEN D7 group showed coagulation necrosis of tubular epithelial cells, degenerated tubules, degenerated epithelial

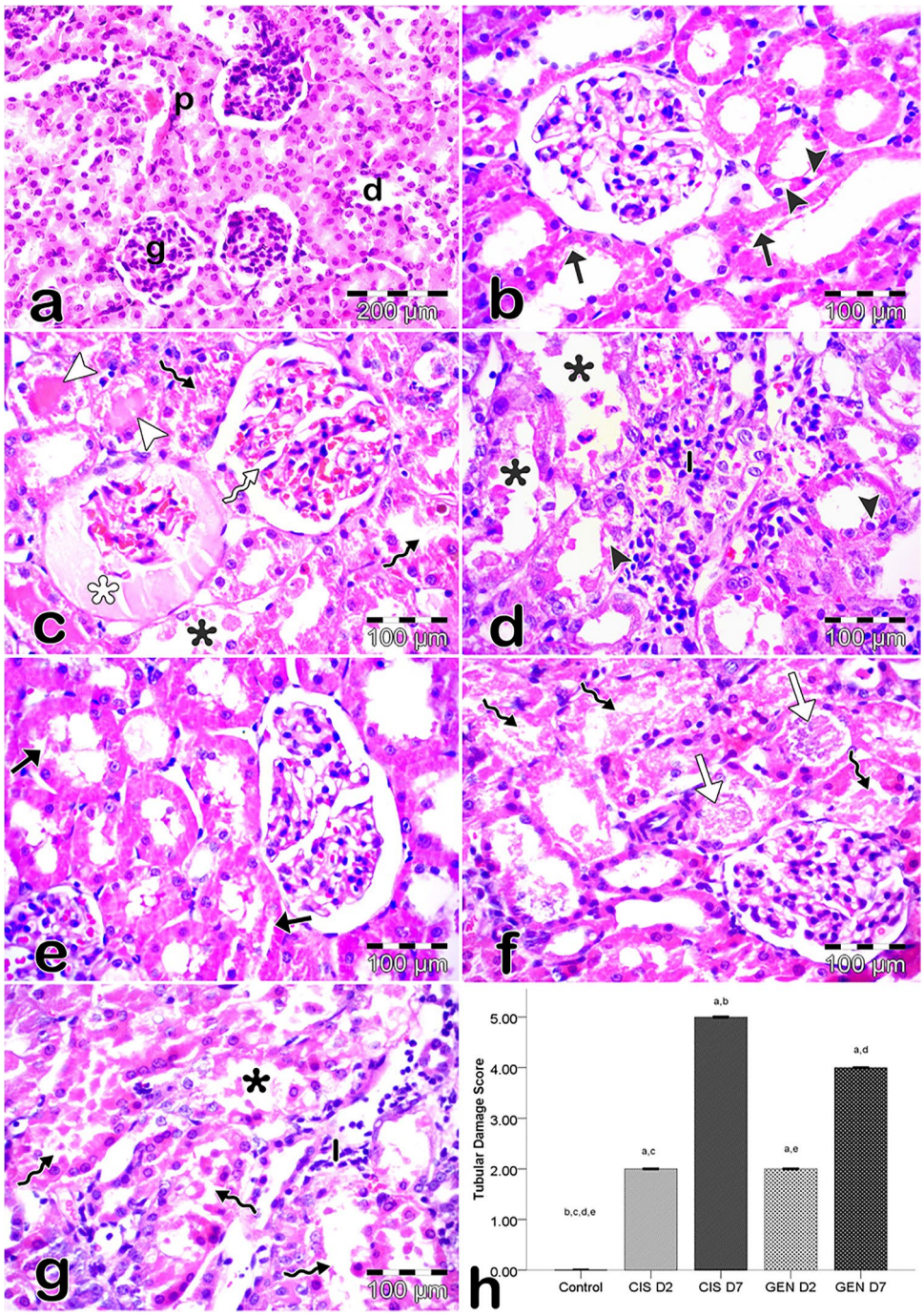


**Fig. 1** Representative photomicrograph of H&E staining. **a** The control group show normal glomeruli (g), proximal (p), and distal (d) tubules (200×). **b** Sections from the CIS D2 group show cellular vacuolation (black arrowheads) and mild degeneration (arrows) in tubule epithelial cells (400×). **c**, **d** Sections from the CIS D7 group show atrophied glomeruli with widening of Bowman's space (white asterisk), glomerular lobulation (white curved arrow), hyaline casts (white arrowheads), debris accumulation in the tubular lumen (black curved arrow), tubular necrosis with sloughed necrotic cells (black asterisks), cellular vacuolation (black arrowheads), and foci of inflammatory cell infiltration (I) (400×). **e** Sections from the GEN D2 group show mild degeneration in tubule epithelial cells (arrows) (400×). **f**, **g** Sections from the GEN D7 group show coagulation necrosis of tubular epithelium (white arrows), interstitial cellular infiltration (I), tubular degeneration (black asterisk), and tubular lumen with sloughed epithelial cells (black curved arrow) (400×). **h** Comparison of tubular damage between groups. Kruskal–Wallis *H* test; a: 0.05; post hoc: Dunn test. [a]The difference between this group and control group was statistically significant. [b]The difference between this group and CIS D2 group was statistically significant. [c]The difference between this group and CIS D7 group was statistically significant. [d]The difference between this group and GEN D2 group was statistically significant. [e]The difference between this group and GEN D7 group was statistically significant. Bar statistics: median; error bars: 95% confidence interval

cells spilled into the tubule lumen, and inflammatory cell infiltration (Fig. 1f, g). Tubular injury scoring was significantly higher in the CIS D7 and GEN D7 groups than that in the control group. When compared to the control group, the difference in the CIS D2 and GEN D2 groups was also statistically significant (Fig. 1h).

## GRP78, PERK, TNF-α, and IL-1β expression

As shown in Figs. 2 and 3, there were few positive cells in the control group when the sections with GRP78 (Fig. 2a) and PERK (Fig. 3a) immunolabeling were examined. CIS D7 (Figs. 2c and 3c) and GEN D7 (Figs. 2e and 3e) groups showed a significant increase in GRP78 and PERK expression in comparison to the control group ($p < 0.05$). The intensity of GRP78 immunoreactivity increased significantly in the CIS D2 (Fig. 2b) and GEN D2 (Fig. 2d) groups compared to the control group; however, the intensity of PERK immunoreactivity increased only in the CIS D2 group ($p < 0.05$, Fig. 3b, f). Although there was an increase in the GEN D2 group, it was not statistically significant ($p > 0.05$, Fig. 3d, f).

As shown in Figs. 4 and 5, CIS D7 and GEN D7 groups showed a significant increase in TNF-α and IL-1β expression in comparison to the control group ($p < 0.05$). The expression of these proteins was also significant in the CIS D2 and GEN D2 groups compared to the control ($p < 0.05$).

## Electron microscopy examinations

The tubular epithelial cells, glomerular basement membrane, glomerular capillaries, and endothelium had typical ultrastructural morphology (Fig. 6a). In the CIS D2 group, irregularity in the glomerular basement membrane, tubule epithelial cell vacuolization, and lysosomal deposits were found in some areas (Fig. 6b). The kidney tissues

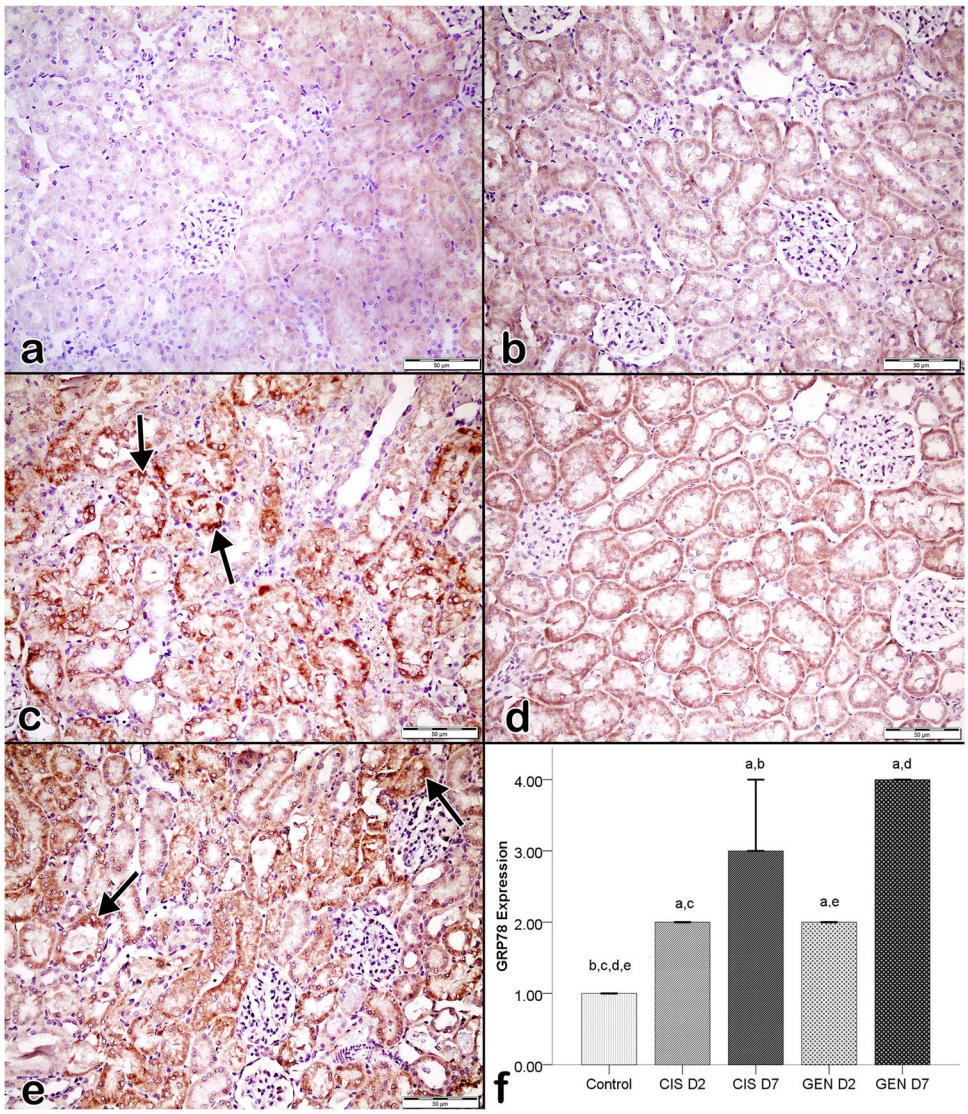


**Fig. 2** Light microscopic image of GRP78 immunoreactivity. **a** Control group sections show few positive cells in tubule epithelial cells (200×). **b** CIS D2 (200×) and **d** GEN D2 (200×) groups show moderate immunostaining cells. **c** CIS D7 (200×) and **e** GEN D7 (200×) groups show intense GRP78 expression (arrows) in tubular epithelium. **f** Comparison of GRP78 expression between groups. Kruskal–Wallis *H* test; a: 0.05; post hoc: Dunn test. [a]The difference between this group and control group was statistically significant. [b]The difference between this group and CIS D2 group was statistically significant. [c]The difference between this group and CIS D7 group was statistically significant. [d]The difference between this group and GEN D2 group was statistically significant. [e]The difference between this group and GEN D7 group was statistically significant. Bar statistics: median; error bars: 95% confidence interval

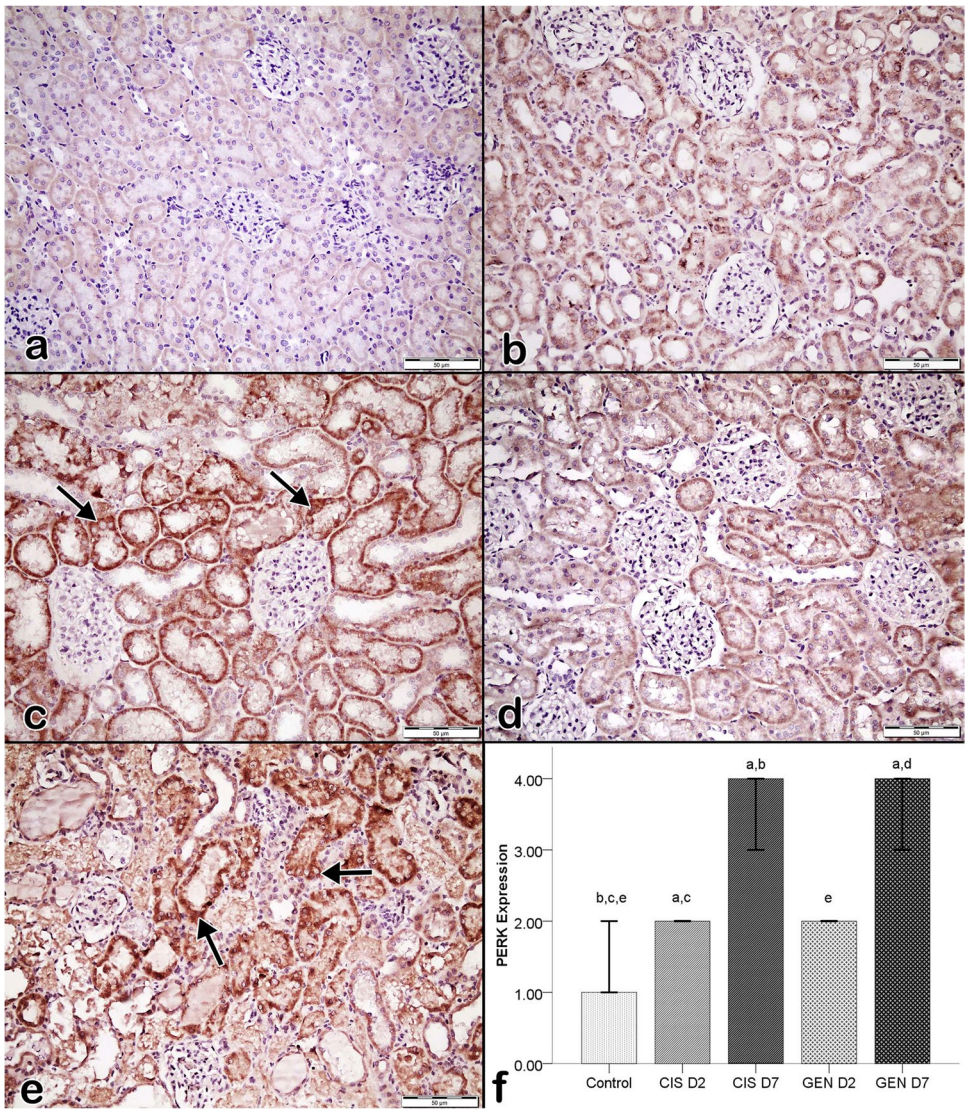


**Fig. 3** Light microscopic image of PERK immunoreactivity. **a** Control group sections show few positive cells in tubule epithelial cells (200×). **b** CIS D2 (200×) and **d** GEN D2 (200×) groups show moderate immunostaining cells. **c** CIS D7 (200×) and **e** GEN D7 (200×) groups show intense PERK expression (arrows) in tubular epithelium. **f** Comparison of PERK expression between groups. Kruskal–Wallis *H* test; a: 0.05; post hoc: Dunn test. [a]The difference between this group and control group was statistically significant. [b]The difference between this group and CIS D2 group was statistically significant. [c]The difference between this group and CIS D7 group was statistically significant. [d]The difference between this group and GEN D2 group was statistically significant. [e]The difference between this group and GEN D7 group was statistically significant. Bar statistics: median; error bars: 95% confidence interval

of the CIS D7 rats showed irregularity and thickening in the glomerular basement membrane, flattening in some pedicels, swelling in the glomerular endothelial cells, and marked irregularity and thickening in the tubule basement membrane, as well as tubular lumen with sloughed cellular material, lysosomal deposits, and increased lipid vacuoles in the tubule epithelial cells, in comparison to the control group (Fig. 6c, d). The GEN D2 group had a focal irregular glomerular basement membrane, mitochondrial swelling, and loss of cristae in tubular epithelial cells (Fig. 6e). When rats in the GEN D7 group were compared to the control group, a focal duplication of the glomerular basement membrane, endocapillary proliferation, and swelling of endothelial cells, as well as enlargement in the intercellular space, vacuolization of tubule cells, lysosomal deposits, increased lipid vacuoles, and ruptured and vague mitochondrial cristae were observed (Fig. 6f).

## Biochemical analysis findings

We measured serum BUN and Cr concentrations 24 h after the last injection to confirm kidney damage caused by CIS and GEN. The CIS D7 and GEN D7 groups had significantly higher BUN and Cr concentrations than did the control group ($p < 0.05$, Table 1). BUN and Cr concentrations in both the CIS D2 and GEN D2 groups, on the other hand, were not significant ($p > 0.05$, Table 1).

As shown in Table 1, when CIS D2 and GEN D2 groups were compared to the control group, there was a statistically insignificant increase in TOS levels ($p < 0.05$). While the TAS level in the CIS D2 group was significantly higher than in the control group ($p < 0.05$), there was no significant increase in GEN D2 ($p > 0.05$). TAS levels decreased in the serum of rats exposed to CIS and GEN for 7 days ($p < 0.05$), while TOS levels increased significantly ($p < 0.05$). We also

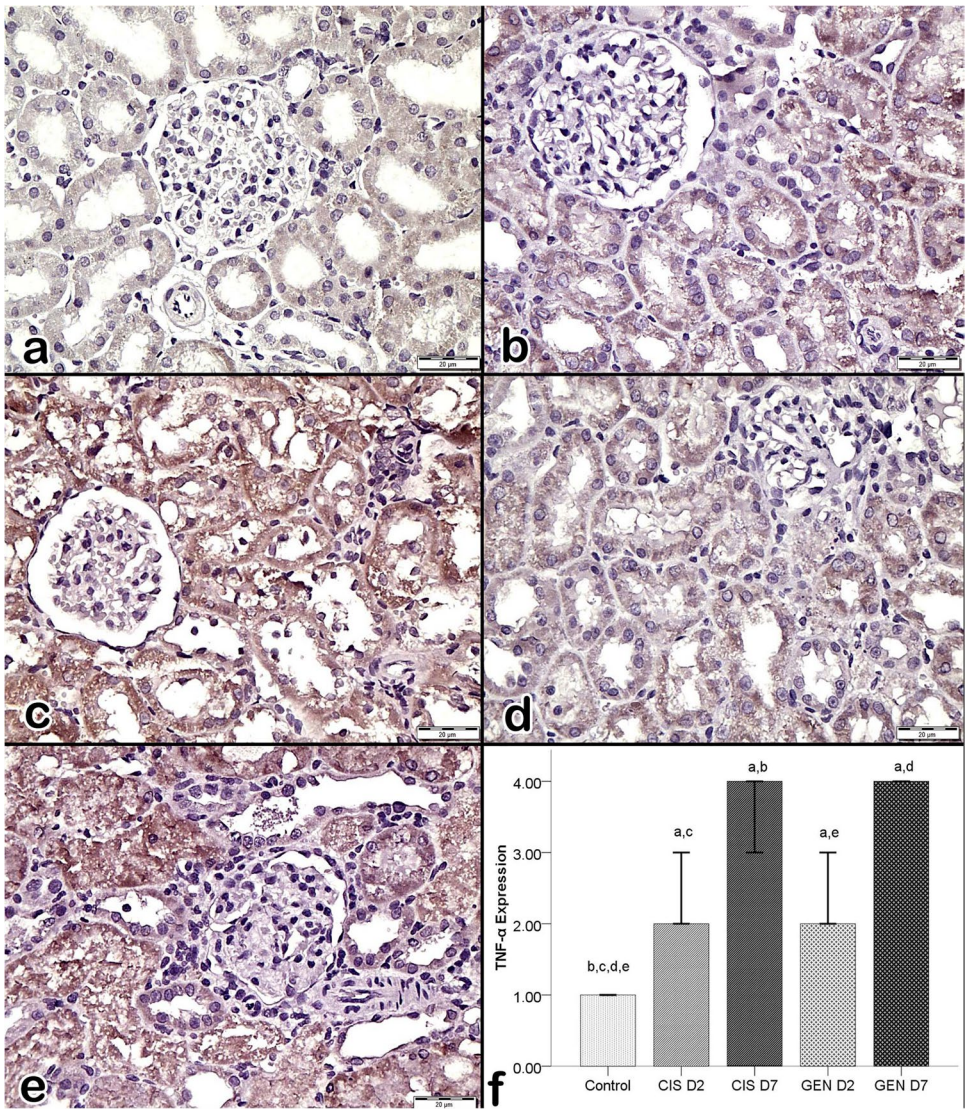


**Fig. 4** Light microscopic image of TNF-α immunoreactivity. **a** Control group sections show few positive cells in tubule epithelial cells (400×). **b** CIS D2 (400×) and **d** GEN D2 (400×) groups show moderate immunostaining cells. **c** CIS D7 (400×) and **e** GEN D7 (400×) groups show intense TNF-α expression in tubular epithelium. **f** Comparison of TNF-α expression between groups. Kruskal–Wallis *H* test; a: 0.05; post hoc: Dunn test. [a]The difference between this group and control group was statistically significant. [b]The difference between this group and CIS D2 group was statistically significant. [c]The difference between this group and CIS D7 group was statistically significant. [d]The difference between this group and GEN D2 group was statistically significant. [e]The difference between this group and GEN D7 group was statistically significant. Bar statistics: median; error bars: 95% confidence interval

found that the CIS D7 TAS levels were significantly lower than those in the CIS D2 group ($p < 0.05$).

## Discussion

Nephrotoxins can cause several problems in the kidneys, from moderate dysfunction to considerable damage and end-stage renal failure. In the workplace or another environment, nephrotoxic chemicals such as heavy metals, organic solvents, and glycols, as well as pesticides, herbicides, and fungicides, can be found. Antiviral, antifungal, antibacterial, antibiotic, and immunosuppressive drugs are only a small part of the many often-used nephrotoxic medications (IPCS 1991; Price 2002). Drug-induced nephrotoxicity continues to be a source of worry, with financial and medical consequences (Izzedine 2018).

CIS is a commonly used anticancer drug for chemotherapy patients, and it is primarily removed by renal clearance. The hydrolysis of CIS is aided by the low chloride content inside the cells. The active species that react with glutathione in the cytoplasm and with DNA in the nucleus have been identified as the hydrolysis product (Boulikas and Vougiouka 2003). As a result, CIS–DNA intrachain crosslinks produce cytotoxicity in cancer cells and other normal proliferating cells (Galea and Murray 2002).

Nephrotoxicity, leading to acute kidney injury, is one of the most well-known serious side effects of CIS (Manohar and Leung 2018). CIS-induced acute kidney injury is mostly transient and reversible but may progress into irreversible chronic kidney disease (Chiruvella et al. 2020). Proximal tubule damage, apoptosis, oxidative stress, and inflammation are all linked to the pathophysiology of CIS (Wang et al. 2018; Ismail et al. 2020). Several studies have suggested that the administration of CIS causes dose-dependent necrosis in

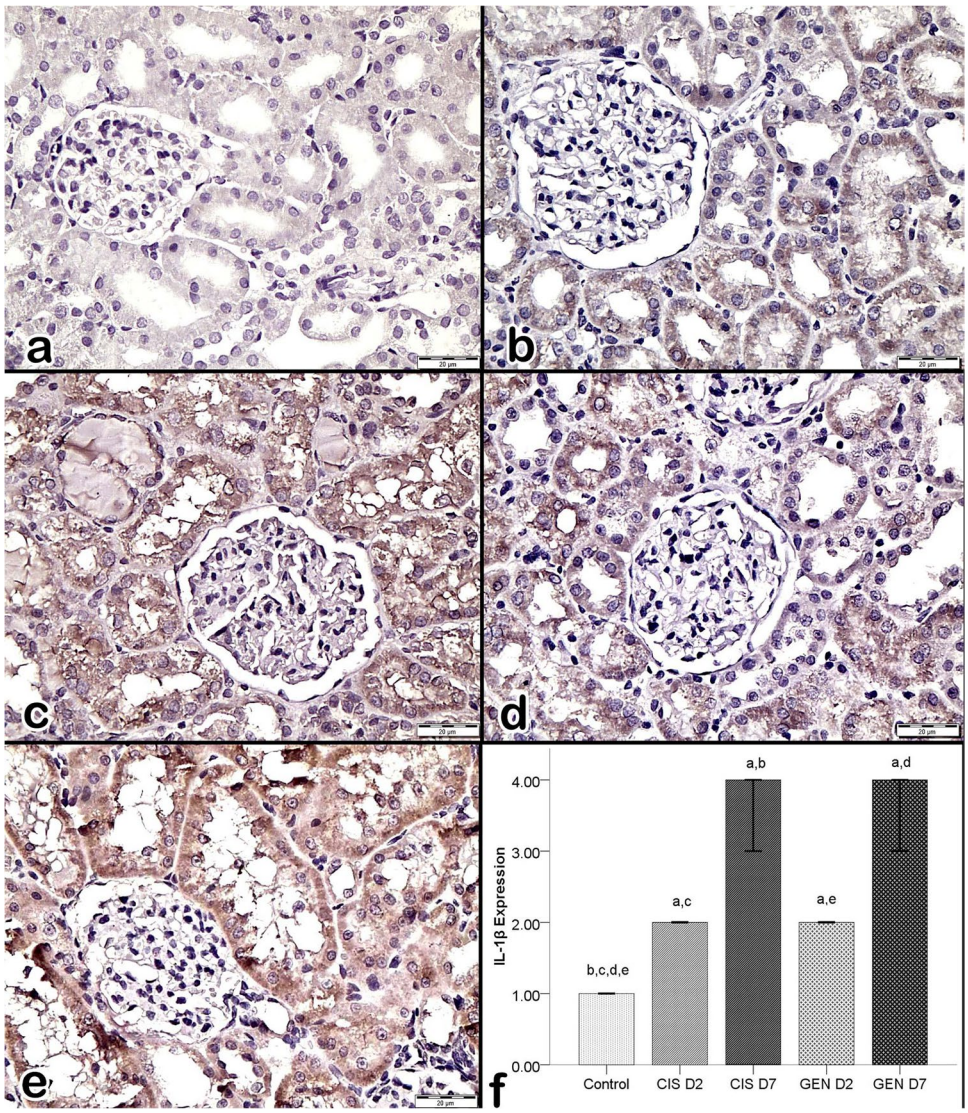


**Fig. 5** Light microscopic image of IL-1β immunoreactivity. **a** Control group sections show few positive cells in tubule epithelial cells (400×). **b** CIS D2 (400×) and **d** GEN D2 (400×) groups show moderate immunostaining cells. **c** CIS D7 (400×) and **e** GEN D7 (400×) groups show intense IL-1β expression in tubular epithelium. **f** Comparison of IL-1β expression between groups. Kruskal–Wallis *H* test; a: 0.05; post hoc: Dunn test. [a]The difference between this group and control group was statistically significant. [b]The difference between this group and CIS D2 group was statistically significant. [c]The difference between this group and CIS D7 group was statistically significant. [d]The difference between this group and GEN D2 group was statistically significant. [e]The difference between this group and GEN D7 group was statistically significant. Bar statistics: median; error bars: 95% confidence interval

proximal tubule cells, debris accumulation in tubules, hyaline casts in tubule lumen, inflammation, and cytoplasmic vacuolization (Gautier et al. 2010; Tomar et al. 2017; Mercantepe et al. 2018). Experimental models of CIS-induced acute kidney injury have revealed increased leukocyte and T-cell infiltration in kidney tissue (Liu et al. 2006). Although our data are consistent with histopathological findings in the literature, the light microscopy examination of the group treated with CIS for 2 days showed minimal degeneration in the proximal tubules. We have found that CIS treatment for 7 days causes some histopathological changes such as necrotic cell debris or degenerated epithelial cells in the tubule lumen, cellular vacuolization, hyaline casts, foci of inflammation containing inflammatory cells, and glomerular atrophy. The histopathological changes caused by the CIS treatment were also assessed using histological scoring as shown in Fig. 1. The destruction of cellular components and/or the release of reactive oxygen (ROS) and free radicals, which cause oxidative damage, could be the origin of the damage we observed in kidney tissues (Hazman et al. 2018; Manohar and Leung 2018).

Focal irregularity and thickening of the glomerular basement membrane, electron-dense deposits in the subendothelial region, atypical podocytes, mitochondrial swelling, ruptured and melted mitochondrial cristae, a large number of lysosomes, and vacuole flattening of the podocyte secondary processes have been previously reported in ultrastructural studies of nephrotoxicity due to CIS (Liu et al. 2015; Mercantepe et al. 2018; Ahmed and Fouad 2019; Kalra et al. 2019). Consistent with the literature, we observed severe tissue damage in kidney samples, particularly in the CIS D7 group, which also supports our light microscopic findings.

Acute kidney injury caused by acute tubular necrosis together with increased Cr concentration is a relatively common side effect of aminoglycoside therapy (McWilliam et al. 2017). Aminoglycoside-induced tubulotoxicity

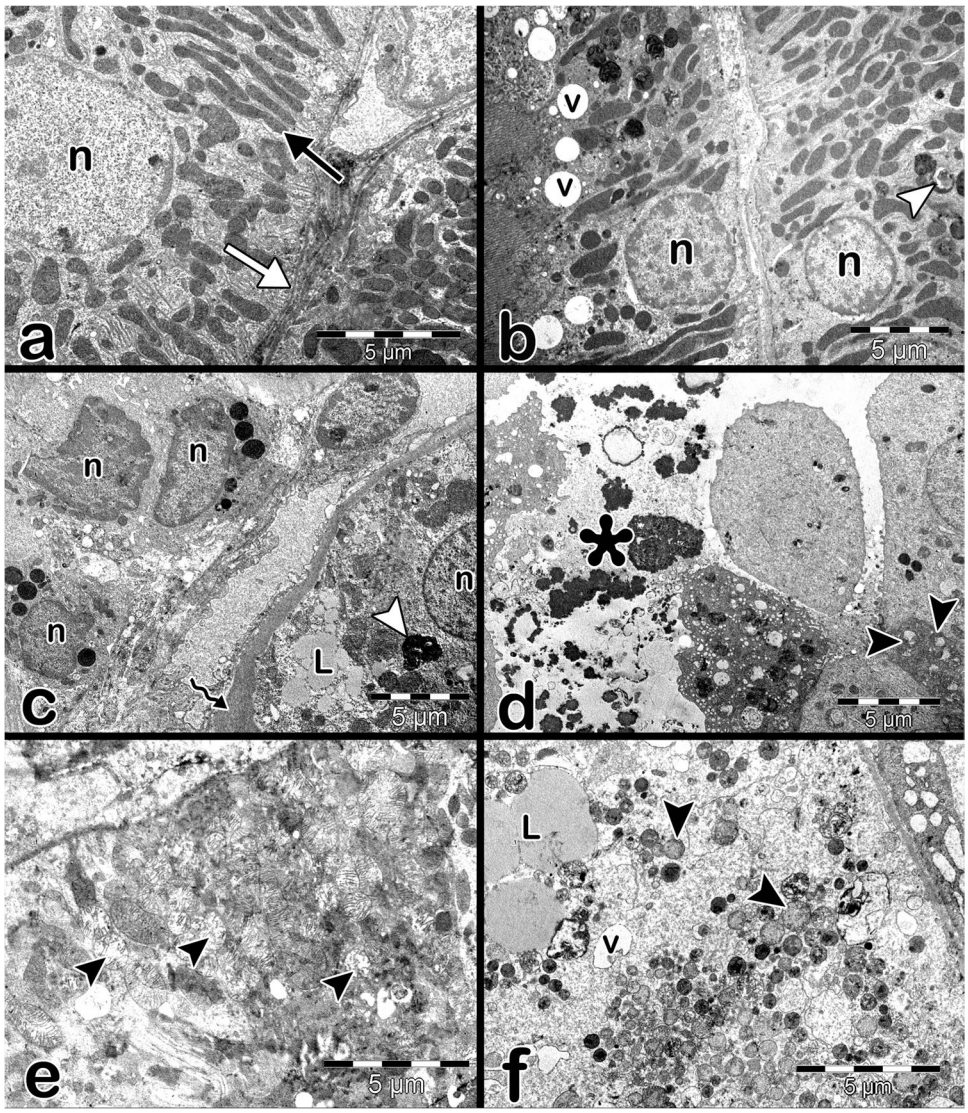


**Fig. 6** Transmission electron microscopic photomicrograph of kidney tissue. **a** Control group micrograph shows a normal tubule basal membrane (white arrow) and mitochondria (black arrow) in tubule epithelial cells (7500×), n: nuclei of tubule epithelial cells. **b** CIS D2 group micrograph shows vacuolization (v) and localized lysosomal deposits (white arrowhead) in the tubule epithelial cells (4000×). **c**, **d** CIS D7 group micrograph shows marked thickening in the tubule basement membrane (curved arrow), increased lipid vacuoles (L), tubular lumen with sloughed cellular material (asterisk), mitochondrial swelling, and loss of cristae (black arrowheads) in some tubular epithelial cells and lysosomal deposits (white arrowhead) (5000×). **e** GEN D2 group micrograph shows swelling and loss of cristae in mitochondria (black arrowheads) (7500×). **f** GEN D7 group micrograph shows vacuolization (v), increased lipid vacuoles (L), and ruptured and vague mitochondrial cristae (black arrowheads) (7500×)

**Table 1** Serum levels of blood BUN, Cr, TAS, and TOS

| Study groups | BUN (mg/dL) | Cr (mg/dL) | TAS (mmol Trolox Eq/L) | TOS (µmol $H_2O_2$ Eq/L) |
|---|---|---|---|---|
| Control | 31.25 ± 2.50 | 0.39 ± 0.07 | 1.46 ± 0.17 | 48.81 ± 12.15 |
| CIS D2 | 19.83 ± 2.64 | 0.42 ± 0.03 | 1.93 ± 0.25[a] | 56.48 ± 41.12 |
| CIS D7 | 281.86 ± 60.72[a,b] | 6.08 ± 2.16[a,b] | 1.18 ± 0.19[a,b] | 159.56 ± 29.58[a,b] |
| GEN D2 | 29.40 ± 5.32 | 0.37 ± 0.05 | 1.42 ± 0.23 | 50.06 ± 9.42 |
| GEN D7 | 159.25 ± 81.45[a,c] | 2.96 ± 1.71[a,c] | 1.20 ± 0.10[a] | 105.67 ± 55.06[a,c] |

One-way ANOVA, post hoc: Tukey HSD test. Results are presented as mean ± SD. Means within the same column with differing superscripts are significantly different ($p < 0.05$)

is reversible by discontinuation of the drug (Girardi et al. 2015). Intracellular accumulation of aminoglycosides is primarily restricted to the S1 and S2 segments of the proximal tubule. However, after renal ischemia, the S3 portion is also a region with high intracellular aminoglycoside concentrations. GEN-induced damage to collecting duct cells has also been observed in animal models (Huang et al. 2020). GEN has been shown to enter proximal tubule cells via endocytosis and accumulate in the Golgi, lysosome, and ER, causing extensive kidney damage depending on the dose and duration of administration (Wargo and Edwards 2014). After binding to the anionic phospholipid of the proximal tubule

cells, the aminoglycosides are immediately transferred to the transmembrane protein megalin and taken up into the cell via endocytosis. Megalin is a cell-surface scavenger receptor with a molecular weight of 600 kDa and exhibits a strong affinity for proteins that contain positively charged amino acid domains. Megalin is highly expressed in many tissues, including the renal proximal tubules, glomerular podocytes, and ciliary and inner ear epithelium (Nagai and Takano 2004). When megalin-mediated endocytosis occurs, endosomes containing aminoglycosides are transferred through the endocytic system and directed to lysosomes and the Golgi complex (Servais et al. 2005). Aminoglycosides migrate retrogradely from the Golgi complex to the ER and ultimately to the cytoplasm. Aminoglycoside molecules in the cytosol accumulate in the nucleus and mitochondria, and thus mitochondrial activity is inhibited (Sandoval and Molitoris 2004).

In the present study, although there was minimal degeneration in the GEN D2 group compared to the control group, histopathological evaluation in the GEN D7 group revealed severe damage such as coagulation necrosis in the tubule epithelial cells, degeneration in the tubule epithelial layer, epithelial cells shed into the tubule lumen, and inflammatory cell infiltration in the kidney tissues. The histopathological changes caused by the GEN treatment were also assessed using histological scoring as shown in Fig. 1. Our results showing GEN-induced nephrotoxicity in rats are consistent with the data in the literature (Sahu et al. 2014; Adil et al. 2016; Katary and Salahuddin 2017). The generation of highly reactive radicals as a result of GEN-induced oxidative stress could be the source of this damage, as shown in Table 1. GEN administration increases monocyte/macrophage infiltration into the site of tissue injury. Neutrophil infiltration causes impaired renal function by secreting ROS, which destroys the glomerular barrier and renal tubular cells. This migration may explain the cellular infiltration we observed here (Bledsoe et al. 2006; Ansari et al. 2016). Severe ultrastructural damage observed in the GEN D7 group is consistent with previously published reports (Abdelsameea et al. 2016; Mahmoud 2017; Abd-Elhamid et al. 2018). GEN disrupts cellular membrane processes by binding to anionic phospholipids, especially mitochondrial phospholipids. Mitochondrial damage leads to an impairment in ATP production and eventually causes cell death (Soliman et al. 2007). The rupture of the lysosomal membrane due to overload releases lysosomal proteases and cathepsins into the cytosol and leads to proteolysis that gives rise to the induction of tubular cell death (Quiros et al. 2011).

As it is well known, elevated levels of BUN and Cr in serum are the two main indicators of renal injury and dysfunction (Schrier et al. 2004). We found that BUN and Cr levels in serum increased after 7 days of CIS and GEN administration compared to the control group, suggesting renal injury in those rats. In the CIS D2 and GEN D2 groups, there was no significant increase. A variety of studies have reported that administering CIS and GEN for 7–8 days increases serum BUN and Cr levels, supporting our findings (Peyrou et al 2007; Sahu et al. 2014; Mahmoud 2017). In these studies, a strong link was found between elevated BUN and Cr levels and histopathological alterations in renal tissue of CIS- and GEN-treated rats (Sahu et al. 2014; Wahdan et al. 2019). The increase in serum BUN and Cr levels is consistent with cell damage in kidney tissue, as shown by light microscopy and TEM.

Previous studies have found that tubular necrosis caused by CIS and GEN stimulates inflammatory reactions in the kidney, resulting in increased migration of neutrophils and monocytes/macrophages to the inflammation site (Balakumar et al. 2010; Miller et al. 2010). Within 72 h following CIS administration, the infiltration of macrophages and leukocytes into renal tissue has been shown to increase (Ueki et al. 2013). TNF-α and IL-1β, two pro-inflammatory cytokines, play an important function in the inflammatory response. Nephrotoxic drugs such as CIS and GEN activate nuclear factor kappa B (NF-κB), increasing the expression of TNF-α and IL-1β in renal tubule cells (Ince et al. 2020; Un et al. 2021). CIS D7 and GEN D7 groups had significantly higher TNF-α and IL-1β expression than that in control group, which is consistent with the literature. This increase may have been a response to the inflammation caused by nephrotoxic drugs like CIS and GEN because during kidney toxicity, injured kidney cells and immune cells produce inflammatory mediators in response to the inflammation caused by nephrotoxic agents. The histological findings of this study, which demonstrated nephrotoxicity in kidney sections of rats administered CIS and GEN for 7 days, support this claim.

As regards the pathophysiological process of nephrotoxicity caused by GEN and CIS, oxidative stress has been suggested to be responsible for the inflammation and ER stress–related damage (Wu et al. 2011; Hazman et al. 2018; Laorodphun et al. 2022). It also causes irreversible damage to macromolecules such as lipid, protein, and DNA by increasing intracellular ROS accumulation, which eventually disrupts ER homeostasis (Gómez-Sierra et al. 2020; Laorodphun et al. 2022). The two nephrotoxic drugs have been shown in recent studies to induce apoptosis by activating multiple ER stress markers (Jaikumkao et al. 2016; Gómez-Sierra et al. 2020; Laorodphun et al. 2022). In this work, rats treated with GEN and CIS for 7 days had statistically higher GRP78 and PERK protein expression in their kidney tissues than rats in the CIS D2 and GEN D2 groups. This increase could be attributed to oxidative stress caused by CIS and GEN disrupting ER homeostasis.

The progression of oxidative stress can be determined by assessing both the rate of oxidant formation and the

levels of all types of antioxidant molecules (Davies 2000). Evaluating TOS and TAS can account for the cumulative and synergistic effects of all oxidant and antioxidant compounds and is a simple way to demonstrate oxidant/antioxidant status (Erel 2005). Previous research has found that when oxidative stress is induced by CIS and GEN, the TOS level increases in the renal tissue while that of TAS decreases (Bami et al. 2017; Hakyemez et al. 2022). In our study, after 7 days of CIS and GEN administration, serum analysis showed that TOS levels increased significantly and TAS levels decreased when compared to the control group, which is consistent with the literature. Under normal circumstances, a physiological balance is present between pro-oxidant species and antioxidant molecules. However, the disruption of this balance in favor of oxidants causes oxidative stress which leads to pathological conditions (Zafar et al. 2019). The production of ROS by CIS and GEN is known to decrease the function of antioxidant enzymes in the kidney (Banday et al. 2008; Nieskens et al. 2018). In this study, we have suggested that the oxidative stress generated by nephrotoxic substances could be the source of imbalance between antioxidants and oxidants, which is in favor of oxidants.

## Conclusion

According to this study, CIS and GEN administration for 7 days causes tissue damage, inflammation, an increase in expression of the ER stress proteins GRP78 and PERK, and an elevation in serum BUN and Cr levels in rat kidney tissue, which could be due to the oxidative stress. Because of these effects, the risk of using these drugs seems to be greater in patients with impaired renal function and in those who receive prolonged therapy. As a result, we can conclude that CIS and GEN should only be used as a short-term induction therapy in an emergency response, and that the related agents should be discontinued after the third day as they will exacerbate kidney damage and therapy should continue with other appropriate and safe drugs. Moreover, since most tubulotoxic damage is transient and reversible, the discontinuation of renally excreted drugs such as CIS and GEN may prevent further iatrogenic kidney damage.

**Author contribution** T.O.M. was in charge of conception and design of the experiment, data collection, execution of the experiment, and paper writing. T.O.M. and S.Y. conducted experiments. B.C.Y., G.B., and T.O.M. carried out histopathological, immunohistochemical, and ultrastructural analyses. N.E., D.A.A., and A.H.K. were involved in adjusting drug doses. A.D. performed statistical analysis. A.Y. set the experimental animal models and L.A. and M.S. contributed to the biochemical analysis and interpretation of findings. The authors declare that all data were generated in-house and that no paper mill was used.

**Funding** This work was supported by Kahramanmaras Sutcu Imam University Department of Scientific Research Projects (grant number: 2017/4–40 M).

**Data availability** The data that support the findings of this study are available on request from the corresponding author.

## Declarations

**Competing interests** The authors declare no competing interests.

**Ethics approval** This present study was approved by Kahramanmaras Sutcu Imam University's local animal experiments ethics committee (approval number: 2017/03–09).

**Conflict of interest** The authors declare no competing interests.

## References

Abd-Elhamid TH, Elgamal DA, Ali SS, Ali FEM, Hassanein EHM, El-Shoura EAM, Hemeida RAM (2018) Reno-protective effects of ursodeoxycholic acid against gentamicin-induced nephrotoxicity through modulation of NF-κB, eNOS and caspase-3 expressions. Cell Tissue Res 374(2):367–387

Abdelsameea AA, Mohamed AM, Amer MG, Attia SM (2016) Cilostazol attenuates gentamicin-induced nephrotoxicity in rats. Exp Toxicol Pathol 68(4):247–253

Adil M, Kandhare AD, Dalvi G, Ghosh P, Venkata S, Raygude KS, Bodhankar SL (2016) Ameliorative effect of berberine against gentamicin-induced nephrotoxicity in rats via attenuation of oxidative stress, inflammation, apoptosis and mitochondrial dysfunction. Ren Fail 38(6):996–1006

Ahmed SM, Fouad FE (2019) Possible protective effect of platelet-rich plasma on a model of cisplatin-induced nephrotoxicity in rats: a light and transmission electron microscopic study. J Cell Physiol 234(7):10470–10480

Amin RP, Vickers AE, Sistare F et al (2004) Identification of putative gene based markers of renal toxicity. Environ Health Perspect 112(4):465–479

Ansari MA, Raish M, Ahmad A, Ahmad SF, Mudassar S, Mohsin K, Shakeel F, Korashy HM, Bakheet SA (2016) Sinapic acid mitigates gentamicin-induced nephrotoxicity and associated oxidative/nitrosative stress, apoptosis, and inflammation in rats. Life Sci 165:1–8

Balakumar P, Rohilla A, Thangathirupathi A (2010) Gentamicin-induced nephrotoxicity: do we have a promising therapeutic approach to blunt it? Pharmacol Res 62(3):179–186

Banday AA, Farooq N, Priyamvada S, Yusufi AN, Khan F (2008) Time dependent effects of gentamicin on the enzymes of carbohydrate metabolism, brush border membrane and oxidative stress in rat kidney tissues. Life Sci 82(9–10):450–459

Bami E, Ozakpınar OB, Ozdemir-Kumral ZN, Köroglu K, Ercan F, Cirakli Z, Sekerler T, Izzettin FV, Sancar M, Okuyan B (2017) Protective effect of ferulic acid on cisplatin induced nephrotoxicity in rats. Environ Toxicol Pharmacol 54:105–111

Bledsoe G, Crickman S, Mao J, Xia CF, Murakami H, Chao L, Chao J (2006) Kallikrein/kinin protects against gentamicin-induced nephrotoxicity by inhibition of inflammation and apoptosis. Nephrol Dial Transplant 21(3):624–633

Boulikas T, Vougiouka M (2003) Cisplatin and platinum drugs at the molecular level. (Review). Oncol Rep 10(6):1663–1682

Chiruvella V, Annamaraju P, Guddati AK (2020) Management of nephrotoxicity of chemotherapy and targeted agents: 2020. Am J Cancer Res 10(12):4151–4164

Davies KJ (2000) Oxidative stress, antioxidant defenses, and damage removal, repair, and replacement systems. IUBMB Life 50(4–5):279–289

Erel O (2005) A new automated colorimetric method for measuring total oxidant status. Clin Biochem 38(12):1103–1111

Foufelle F, Fromenty B (2016) Role of endoplasmic reticulum stress in drug-induced toxicity. Pharmacol Res Perspect 4(1):e00211

Galea AM, Murray V (2002) The Interaction of Cisplatin and Analogues with DNA in Reconstituted Chromatin. Biochim Biophys Acta 1579(2–3):142–152

Gautier JC, Riefke B, Walter J et al (2010) Evaluation of novel biomarkers of nephrotoxicity in two strains of rat treated with cisplatin. Toxicol Pathol 38(6):943–956

Ghosh S (2019) Cisplatin: the first metal based anticancer drug. Bioorg Chem 88:102925

Girardi A, Raschi E, Galletti S, Poluzzi E, Faldella G, Allegaert K, De Ponti F (2015) Drug-induced renal damage in preterm neonates: state of the art and methods for early detection. Drug Saf 38(6):535–551

Gómez-Sierra T, Medina-Campos ON, Solano JD, Ibarra-Rubio ME, Pedraza-Chaverri J (2020) Isoliquiritigenin pretreatment induces endoplasmic reticulum stress-mediated hormesis and attenuates cisplatin-induced oxidative stress and damage in LLC-PK1 cells. Molecules 25(19):4442

Hakyemez IN, Cevizci MN, Aksoz E, Yilmaz K, Uysal S, Altun E (2022) Protective effects of *p*-coumaric acid against gentamicin-induced nephrotoxicity in rats. Drug Chem Toxicol 45(6):2825–2832

Hazman Ö, Bozkurt MF, Fidan AF, Uysal FE, Çelik S (2018) The effect of boric acid and borax on oxidative stress, inflammation, ER stress and apoptosis in cisplatin toxication and nephrotoxicity developing as a result of toxication. Inflammation 41(3):1032–1048

Huang H, Jin WW, Huang M, Ji H, Capen DE, Xia Y, Yuan J, Păunescu TG, Lu HAJ (2020) Gentamicin-induced acute kidney injury in an animal model involves programmed necrosis of the collecting duct. J Am Soc Nephrol 31(9):2097–2115

Inagi R (2009) Endoplasmic reticulum stress in the kidney as a novel mediator of kidney injury. Nephron Exp Nephrol 112(1):e1-9

IPCS (International Programme on Chemical Safety) (1991) Principles and methods for the assessment of nephrotoxicity associated with exposure to chemicals. WHO Geneva Environ Health Criteria 119:1–266

Ince S, Kucukkurt I, Demirel HH, Arslan-Acaroz D, Varol N (2020) Boron, a trace mineral, alleviates gentamicin-induced nephrotoxicity in rats. Biol Trace Elem Res 195(2):515–524

Ismail RS, El-Awady MS, Hassan MH (2020) Pantoprazole abrogated cisplatin-induced nephrotoxicity in mice via suppression of inflammation, apoptosis, and oxidative stress. Naunyn Schmiedebergs Arch Pharmacol 393(7):1161–1171

Izzedine H (2018) Drug nephrotoxicity. Nephrol Ther 14(3):127–134

Jaikumkao K, Pongchaidecha A, Thongnak LO, Wanchai K, Arjinajarn P, Chatsudthipong V, Chattipakorn, (2016) Amelioration of renal inflammation, endoplasmic reticulum stress and apoptosis underlies the protective effect of low dosage of atorvastatin in gentamicin-induced nephrotoxicity. PLoS ONE 11(10):e0164528

Kalra P, Karwasra R, Gupta YK, Ray SB, Singh S (2019) Terminalia chebula supplementation attenuates cisplatin-induced nephrotoxicity in Wistar rats through modulation of apoptotic pathway. Nat Prod Res 33(11):1641–1645

Katary M, Salahuddin A (2017) Ameliorative effect of gossypin against gentamicin-induced nephrotoxicity in rats. Life Sci 176:75–81

Laorodphun P, Cherngwelling R, Panya A, Arjinajarn P (2022) Curcumin protects rats against gentamicin-induced nephrotoxicity by amelioration of oxidative stress, endoplasmic reticulum stress and apoptosis. Pharm Biol 60(1):491–500

Liu M, Chien CC, Burne-Taney M, Molls RR, Racusen LC, Colvin RB, Rabb H (2006) A pathophysiologic role for T lymphocytes in murine acute cisplatin nephrotoxicity. J Am Soc Nephrol 17(3):765–774

Liu X, Huang Z, Zou X, Yang Y, Qiu Y, Wen Y (2015) Possible mechanism of PNS protection against cisplatin-induced nephrotoxicity in rat models. Toxicol Mech Methods 25(5):347–354

Mahmoud YI (2017) Kiwi fruit (Actinidia deliciosa) ameliorates gentamicin-induced nephrotoxicity in albino mice via the activation of Nrf2 and the inhibition of NF-κB (Kiwi&gentamicin-induced nephrotoxicity). Biomed Pharmacother 94:206–218

Malik S, Suchal K, Gamad N, Dinda AK, Arya DS, Bhatia J (2015) Telmisartan ameliorates cisplatin-induced nephrotoxicity by inhibiting MAPK mediated inflammation and apoptosis. Eur J Pharmacol 748:54–60

Manohar S, Leung N (2018) Cisplatin nephrotoxicity: a review of the literature. J Nephrol 31(1):15–25

McWilliam SJ, Antoine DJ, Smyth RL, Pirmohamed M (2017) Aminoglycoside-induced nephrotoxicity in children. Pediatr Nephrol 32(11):2015–2025

Mercantepe F, Mercantepe T, Topcu A, Yılmaz A, Tumkaya L (2018) Protective effects of amifostine, curcumin, and melatonin against cisplatin-induced acute kidney injury. Naunyn Schmiedebergs Arch Pharmacol 391(9):915–931

Miller RP, Tadagavadi RK, Ramesh G, Reeves WB (2010) Mechanisms of Cisplatin Nephrotoxicity. Toxins (Basel) 2(11):2490–2518

Nagai J, Takano M (2004) Molecular aspects of renal handling of aminoglycosides and strategies for preventing the nephrotoxicity. Drug Metab Pharmacokinet 19(3):159–170

Nieskens TTG, Peters JGP, Dabaghie D, Korte D, Jansen K, Van Asbeck AH, Tavraz NN, Friedrich T, Russel FGM, Masereeuw R, Wilmer MJ (2018) Expression of organic anion transporter 1 or 3 in human kidney proximal tubule cells reduces cisplatin sensitivity. Drug Metab Dispos 46(5):592–599

Ozcicek A, Ozcicek F, Cimen FK, Mammadov R, Cankaya M, Ezmeci T, Altuner D (2018) The effect of anakinra to nephrotoxicity with cisplatin induced in rats: biochemical, gene expression and histopathological evaluation. Adv Clin Exp Med 27(12):1643–1650

Peyrou M, Hanna PE, Cribb AE (2007) Cisplatin, gentamicin, and p-aminophenol induce markers of endoplasmic reticulum stress in the rat kidneys. Toxicol Sci 99(1):346–353

Price RG (2002) Early markers of nephrotoxicity. Comp Clin Path 11:2–7

Quiros Y, Vicente-Vicente L, Morales AI, López-Novoa JM, López-Hernández FJ (2011) An integrative overview on the mechanisms underlying the renal tubular cytotoxicity of gentamicin. Toxicol Sci 119(2):245–256

Sahu BD, Tatireddy S, Koneru M, Borkar RM, Kumar JM, Kuncha M, Srinivas R, Shyam Sunder R, Sistla R (2014) Naringin ameliorates gentamicin-induced nephrotoxicity and associated mitochondrial dysfunction, apoptosis and inflammation in rats: possible mechanism of nephroprotection. Toxicol Appl Pharmacol 277(1):8–20

Sandoval RM, Molitoris BA (2004) Gentamicin traffics retrograde through the secretory pathway and is released in the cytosol via the endoplasmic reticulum. Am J Physiol Renal Physiol 286(4):F617-624

Schrier RW, Wang W, Poole B, Mitra A (2004) Acute renal failure: definitions, diagnosis, pathogenesis, and therapy. J Clin Invest 114(1):5–14

Servais H, Van Der Smissen P, Thirion G, Van der Essen G, Van Bambeke F, Tulkens PM, Mingeot-Leclercq MP (2005)

Gentamicin-induced apoptosis in LLC-PK1 cells: involvement of lysosomes and mitochondria. Toxicol Appl Pharmacol 206(3):321–333

Singh MP, Chauhan AK, Kang SC (2018) Morin hydrate ameliorates cisplatin-induced ER stress, inflammation and autophagy in HEK-293 cells and mice kidney via PARP-1 regulation. Int Immunopharmacol 56:156–167

Soliman KM, Abdul-Hamid M, Othman AI (2007) Effect of carnosine on gentamicin-induced nephrotoxicity. Med Sci Monit 13(3):BR73-83

Tomar A, Vasisth S, Khan SI, Malik S, Nag TC, Arya DS, Bhatia J (2017) Galangin ameliorates cisplatin induced nephrotoxicity in vivo by modulation of oxidative stress, apoptosis and inflammation through interplay of MAPK signaling cascade. Phytomedicine 34:154–161

Ueki M, Ueno M, Morishita J, Maekawa N (2013) Curcumin ameliorates cisplatin-induced nephrotoxicity by inhibiting renal inflammation in mice. J Biosci Bioeng 115(5):547–551

Un H, Ugan RA, Gurbuz MA, Bayir Y, Kahramanlar A, Kaya G, Cadirci E, Halici Z (2021) Phloretin and phloridzin guard against cisplatin-induced nephrotoxicity in mice through inhibiting oxidative stress and inflammation. Life Sci 266:118869

Vysakh A, Abhilash S, Kuriakose J, Midhun SJ, Jyothis M, Latha MS (2018) Protective effect of Rotula aquatica Lour against gentamicin induced oxidative stress and nephrotoxicity in Wistar rats. Biomed Pharmacother 106:1188–1194

Wahdan SA, Azab SS, Elsherbiny DA, El-Demerdash E (2019) Piceatannol protects against cisplatin nephrotoxicity via activation of Nrf2/HO-1 pathway and hindering NF-κB inflammatory cascade. Naunyn Schmiedebergs Arch Pharmacol 392(11):1331–1345

Wang SW, Xu Y, Weng YY, Fan XY, Bai YF, Zheng XY, Lou LJ, Zhang F (2018) Astilbin ameliorates cisplatin-induced nephrotoxicity through reducing oxidative stress and inflammation. Food Chem Toxicol 114:227–236

Wargo KA, Edwards JD (2014) Aminoglycoside-Induced Nephrotoxicity. J Pharm Pract 27(6):573–577

Wei XM, Jiang S, Li SS, Sun YS, Wang SH, Liu WC, Wang Z, Wang YP, Zhang R, Li W (2021) Endoplasmic reticulum stress-activated PERK-eIF2α-ATF4 signaling pathway is involved in the ameliorative effects of ginseng polysaccharides against cisplatin-induced nephrotoxicity in mice. ACS Omega 6(13):8958–8966

Wu CT, Sheu ML, Tsai KS, Chiang CK, Liu SH (2011) Salubrinal, an eIF2α dephosphorylation inhibitor, enhances cisplatin-induced oxidative stress and nephrotoxicity in a mouse model. Free Radic Biol Med 51(3):671–680

Xu Y, Ma H, Shao J, Wu J, Zhou L, Zhang Z, Wang Y, Huang Z, Ren J, Liu S, Chen X, Han J (2015) A role for tubular necroptosis in cisplatin-induced AKI. J Am Soc Nephrol 26(11):2647–2658

Yao X, Panichpisal K, Kurtzman N, Nugent K (2007) Cisplatin nephrotoxicity: a review. Am J Med Sci 334(2):115–124

Zafar MS, Quarta A, Marradi M, Ragusa A (2019) Recent developments in the reduction of oxidative stress through antioxidant polymeric formulations. Pharmaceutics 11(10):505

Zhao X, Zhang G, Wu L, Tang Y, Guo C (2021) Inhibition of ER stress-activated JNK pathway attenuates TNF-α-induced inflammatory response in bone marrow mesenchymal stem cells. Biochem Biophys Res Commun 541:8–14